JOURNAL OF CATALYSIS 67, 35–48 (1981)

Photoassisted Heterogeneous Catalysis: Rate Equations for Oxidation of 2-Methyl-2-butyl-alcohol and Isobutane

LORETTE PRUDEN CHILDS[1] AND DAVID F. OLLIS[2]

Department of Chemical Engineering, Princeton University, Princeton, New Jersey 08544

Received December 26, 1979; revised June 4, 1980

Rate equations are presented for the photoassisted catalytic oxidation to acetone of 2-methyl-2-butyl-alcohol and isobutane over titanium dioxide catalysts. The alcohol oxidation rate can be described by an expression reflecting a single rate-determining step: the two-site dehydration of adsorbed alcohol. The rate of isobutane oxidation is presumed to be controlled by two surface steps in series: (i) formation of and (ii) subsequent dehydration of an alcohol intermediate. The rate equation derived from these assumptions represents the data satisfactorily when all sites are taken as identical. These model results indicate that dissociated oxygen participates in the photocatalytic alkane oxidation.

INTRODUCTION

Of the many reactions claimed to be photocatalyzed heterogeneously (*1*), the partial oxidation of alkanes and alcohols by titanium dioxide has been studied most extensively (*2–12*). Under illumination of band-gap (~350 nm) or greater energy, at near-ambient temperatures, TiO_2 is a photoassisted catalyst for the reaction of oxygen with alkanes or alcohols to form aldehydes and ketones (*4, 8*) as well as water and carbon dioxide:

$$n\text{-}C_nH_{2n+2} + O_2 \xrightarrow[TiO_2]{h\nu} C_mH_{2m}O,\ C_nH_{2n}O \quad \text{for } [2 < m < n] \quad (1a)$$

$$\text{branched } C_nH_{2n+2} + O_2 \xrightarrow[TiO_2]{h\nu} C_m2_{2m}O \quad \text{for } [3 \leq m < n] \quad (1b)$$

$$n\text{-}C_nH_{2n+1}OH + O_2 \xrightarrow[TiO_2]{h\nu} C_mH_{2m}O,\ C_nH_{2n}O \quad \text{for } [2 < m < n] \quad (2a)$$

$$\text{branched-}C_nH_{2n+1}OH + O_2 \xrightarrow[TiO_2]{h\nu} C_mH_{2m}O \quad \text{for } [3 \leq m < n] \quad (2b)$$

Teichner and co-workers (*4, 6–8*) have suggested that the oxidation of secondary and tertiary alkanes involves, as a first step, the insertion of an (undetected) atomic oxygen into the bond between hydrogen and a secondary or tertiary carbon to form the corresponding alcohol. These workers argued that dehydration of the alcohol to an olefin intermediate is the only step which accounts for the lower aldehydes and ketones noted as final oxidation products.

The existence of olefin intermediate is supported by the work of Carrisoza and Munuera (*13, 14*). They showed that, under nonoxidizing conditions, thermal dehydration of aliphatic alcohols on TiO_2 (anatase) yields water and the corresponding olefins. Inhibition of oxygen isotopic exchange by isobutane oxidation over irradiated TiO_2 implied that these reactions involved the same intermediate. It was therefore inferred that a dissociated oxygen species participates in the alkane oxidation (*15*).

The plausibility of the mechanistic scheme of Teichner *et al.* is tested in this paper by comparing experimental rate data

[1] Present address: Mobil Research and Development Corp. P.O. Box 1025, Princeton, NJ 08540.

[2] Present address: Dept. of Chemical Engineering University of California, Davis, CA 95616.

0021-9517/81/010035-14$02.00/0

to appropriate rate expressions, using the existing data for photoassisted catalytic oxidation of isobutane and 2-methyl-2-butyl-alcohol.

DATA FOR ALCOHOL AND ISOALKANE OXIDATION, AND PRIOR RATE MODELS

Detailed kinetic data are reported in the photooxidation study of Formenti *et al.* (*7*) concerning isobutane conversion to acetone, an example of reaction (1b) above. In a steady-state, fixed bed flow reactor at 30°C, the rate of acetone formation was measured as a function of oxygen and isobutane partial pressures. A subsequent study at 95°C by Walker *et al.* (*9*) yielded the rate of acetone formation from the tertiary alcohol 2-methyl-2-butyl-alcohol, again as a function of both reactant pressures. The alcohol results are summarized in Figs. 1a and b. The isobutane results are presented as inverse rate versus inverse pressure of each reactant in Figs. 2a, b, and c.

A rate equation for the isobutane data was derived by Formenti *et al.*, following earlier arguments of Hinshelwood (*16*) and Downie *et al.* (*17–29*), by assuming that

(a) the adsorption rate for oxygen was given by

$$r_{\text{adsorption}} = k_O P_O{}^N(1 - \theta_O) \qquad (3)$$

(b) oxygen desorption was negligible (below 300°C), and

(c) the hydrocarbon was physisorbed (no chemisorption of isobutane was observed) in a Langmuir fashion with its coverage given by

$$\theta_C = \frac{K_C P_C}{1 + K_C P_C} \qquad (4)$$

The rate of acetone formation was taken to be proportional to $\theta_O\theta_C$, and oxygen consumption was assumed to be proportional to acetone formation; hence

$$r_{\text{consumption}} = k_r\theta_O\theta_C \qquad (5)$$

Equating rates at steady state,

$$r_{\text{adsorption}} = r_{\text{consumption}},$$

gave the rate expression (*6*)

$$r = \frac{k_r K_C k_O P_C P_O{}^N}{k_r K_C P_C + k_O P_O{}^N(1 + K_C P_C)} \qquad (6)$$

This form was the same as that derived by Mars and van Kevelen (*21*) from a surface oxidation/reduction model for hydrocarbon oxidations on oxide catalysts with no illumination. Inversion gave Eq. (7):

$$\frac{1}{r} = \frac{1}{k_O P_O{}^N} + \frac{1}{K_r K_C P_C} + \frac{1}{k_r}. \qquad (7)$$

In our view, this derivation suffers from three weaknesses:

(a) The resulting Eq. (7) predicts that plots of $1/r$ versus $1/P_O{}^N$ (where $N = 1$ or $\frac{1}{2}$) and of $1/r$ versus $1/P_C$ should produce lines of constant slope, independent of the pressure of the second reactant. These predictions are in clear disagreement with Fig. 2.

(b) The form of the adsorption rate expression is incorrect if $N = \frac{1}{2}$, indicating dissociative oxygen adsorption. The form should include $P_O(1 - \theta_O)^2$, not $P_O{}^{1/2}(1 - \theta_O)$.

(c) The original rate expression for irreversible oxygen adsorption (Eq. 3) was proposed because no subsequent desorption of molecular oxygen was observed. However, this latter experimental result might be expected if the total oxygen uptake is small. Such could be the case if

(1) the number of active sites were small, and/or

(2) oxygen adsorption involved depletive chemisorption on *n*-type TiO_2 (*22*), that is, $O_2(g) \rightarrow O^-_{2(ads)}$.

An empirical rate expression for isobutane oxidation was recently suggested (*10*) as

$$r_{\text{acetone}} = kP_O{}^m P_C{}^n \qquad (8)$$

where $m = 0$ and $n = 0.35$ for oxygen and isobutane partial pressures from 100 to 500 Torr.

Such empirical reaction orders may vary with intensity of uv illumination as well as partial pressure of reactants: the apparent values of n for isobutane are 0.45 and 0.68

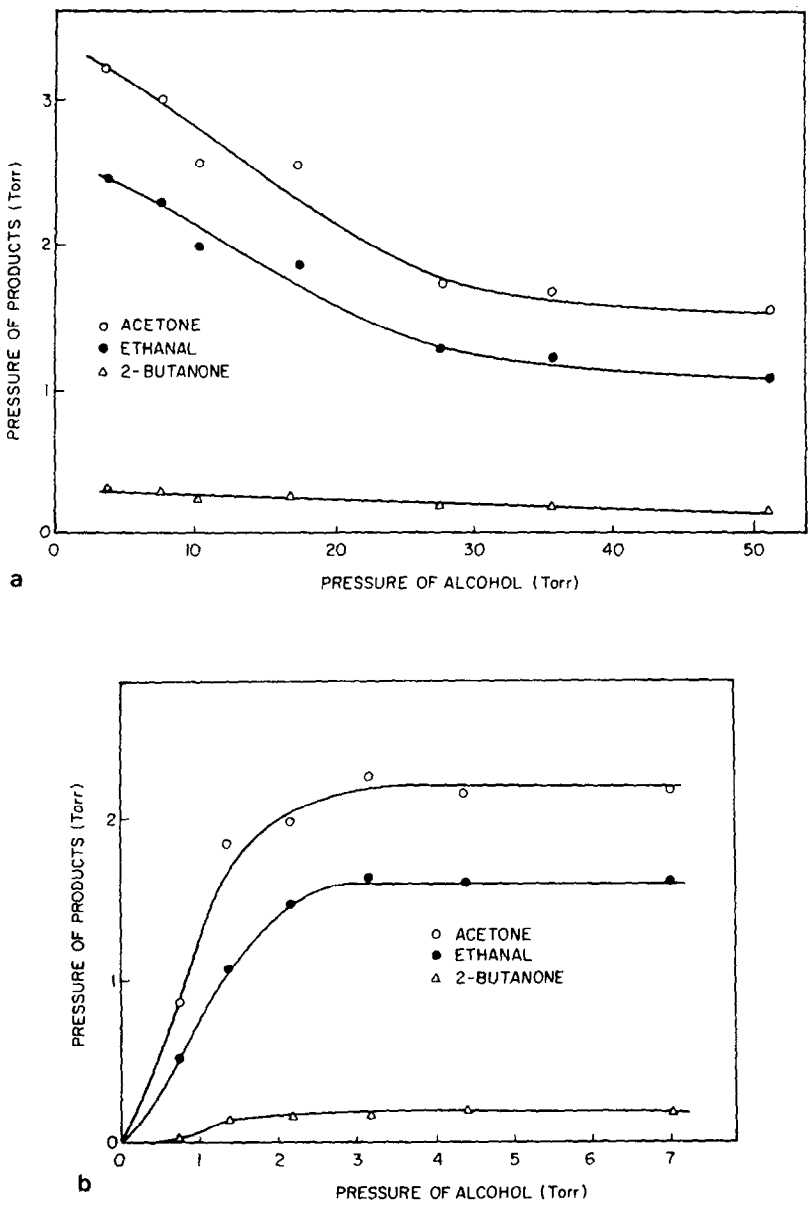

FIG. 1. Partial pressures of 2-methyl-2-butyl-alcohol oxidation products vs alcohol partial pressure (Ref. 9). (a) P_0 = 380 Torr; (b) P_0 = 608 Torr.

t the two (unspecified) intensities of Ref. 7). Also, the rate of acetone production is learly dependent on oxygen pressures elow 100 Torr (7). A smaller positive ıfluence of oxygen on acetone rate is noted ı the data of Fig. 1, Ref. (10). Different atalyst preparations and pretreatment may lso account for some of the differences in xygen pressure dependencies reported in efs. (7) and (10).

Suitable rate expressions, either mechanistically or empirically based, are obviously lacking. Hence it is reasonable to examine rate expressions which are derived from plausible adsorption functions and existing mechanistic information. Recent simultaneous measurements of acetone production and catalyst conductivity indicate that uv-generated holes and electrons react with adsorbed oxygen to form an atomic oxygen species (10). In the following discussion, we will assume that the

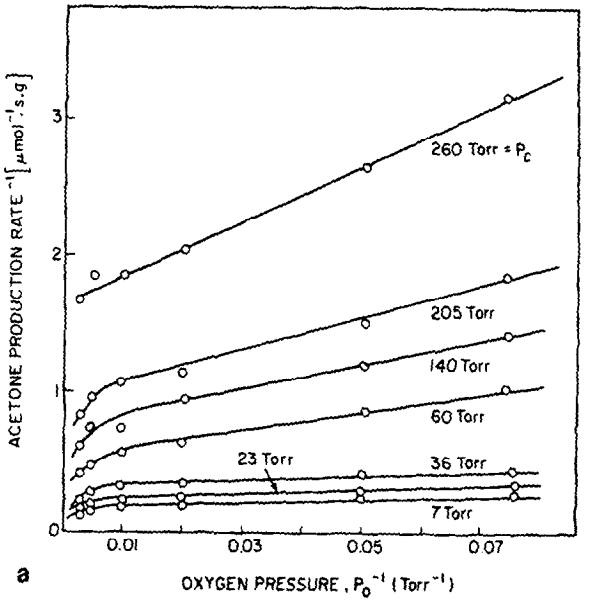
ACETONE PRODUCTION RATE $^{-1}$ [μmol^{-1}.s.g]
260 Torr = P_c
205 Torr
140 Torr
60 Torr
23 Torr
36 Torr
7 Torr
0.01
0.03
0.05
0.07
OXYGEN PRESSURE, P_o^{-1} (Torr^{-1})

a

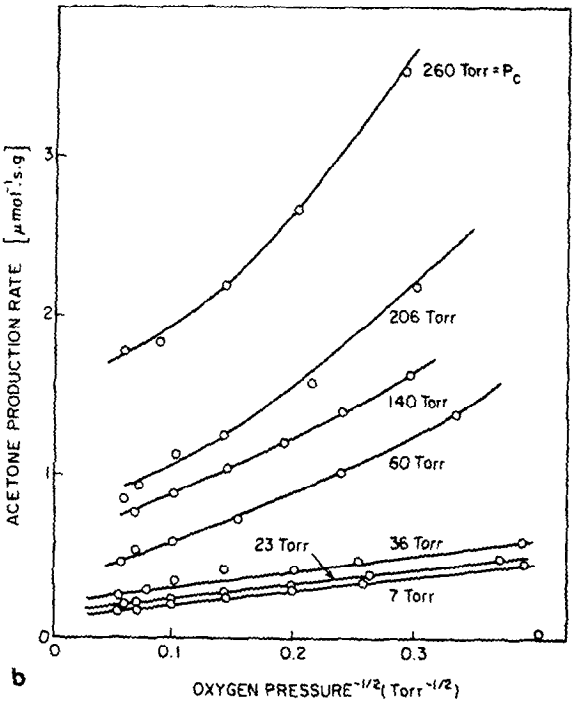
ACETONE PRODUCTION RATE [μmol^{-1}.s.g]
260 Torr = P_c
206 Torr
140 Torr
60 Torr
23 Torr
36 Torr
7 Torr
0.1
0.2
0.3
OXYGEN PRESSURE$^{-1/2}$ (Torr$^{-1/2}$)

b

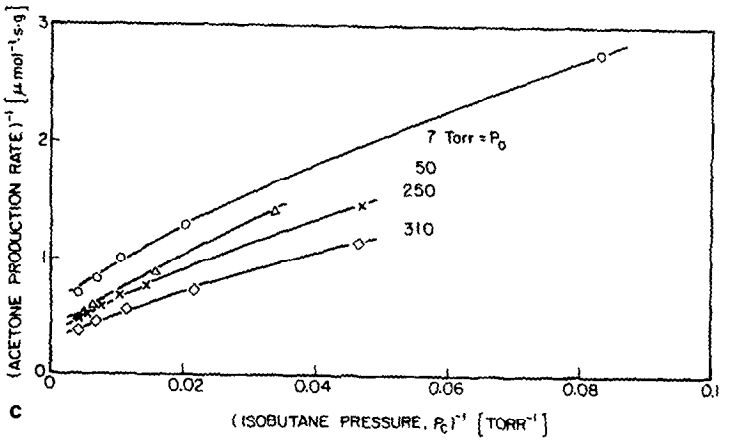
(ACETONE PRODUCTION RATE)$^{-1}$ [μmol^{-1}.s.g]
7 Torr = P_o
50
250
310
0.02
0.04
0.06
0.08
0.1
(ISOBUTANE PRESSURE, P_c)$^{-1}$ [TORR^{-1}]

c

TABLE I

Presumed Reaction Schemes[a]

Alcohol	Isoalkane
(1) $R_2COHR'(g) + S \overset{K_{OH}}{\rightleftarrows} (R_2COHR' \cdot S)$	(1) $R_2CHR'(g) + S \overset{K_i}{\rightleftarrows} (R_2CHR' \cdot S)$
(2) $2\,S + O_2 \overset{K_0}{\rightleftarrows} 2(O \cdot S)$	(2) $2\,S + O_2 \overset{k_0}{\rightleftharpoons} 2(O \cdot S)$
(3) $(R_2COHR' \cdot S) + S \overset{k_r}{\rightarrow} ((R_2C = R') \cdot S) + (H_2O \cdot S)$	(3a) $(R_2CHR' \cdot S) + (O \cdot S) \underset{k_{-3}}{\overset{k_3}{\rightleftarrows}} (R_2COHR' \cdot S) + S$
(3') $(R_2COHR' \cdot S) + S \overset{k_r'}{\rightarrow} (R = C(R)R' \cdot S) + (H_2O \cdot S)$	(3b) $(R_2COHR' \cdot S) + S \underset{k_4}{\rightarrow} [(R_2C = R') \cdot S] + (H_2O \cdot S)$
further reactions (rapid)	
(4) $R_2C = R' + O_2 \rightarrow R_2C = O + O = R'$	
(5) $O = R' \rightarrow$ desorbed product (if $R' > CH_2$)	
$\rightarrow CO_2 + H_2O$ (if $R' = CH_2$)	

[a] R = CH_3; R' = C_2H_5 (alcohol), = CH_3 (isoalkane).

coverage of this presumed active species can be described by a "pseudoequilibrium" "isotherm", i.e., that hole/electron transport is rapid compared with adsorption and reaction.

DERIVATION OF NEW MODEL AND COMPARISON WITH EXPERIMENTS

Teichner and co-workers have shown experimentally that the rates of acetone formation from isobutane or isobutanol are comparable, while the rate from the presumed but undetected intermediate isobutene is higher (*5*). Thus the kinetically slow step in oxidation of either the hydrocarbon or the alcohol involves the same reaction, presumably the surface dehydration of the observed alcohol species (*5, 7, 8*). The low selectivity of isobutane to *t*-butyl-alcohol (9%) in the gas phase relative to acetone (61%) implies that the rate of formation of the alcohol intermediate is similar to the rate of conversion to acetone via dehydration and subsequent olefin oxidation (*5*).

We have assumed, for simplicity, that the rates of alcohol formation and dehydration are equal, and that the dehydration step requires an adjacent vacant site so that both products, olefin and water, may be accommodated on the surface. The proposed surface reaction scheme is shown in Table 1.

The specific nature of the adsorption sites for hydrocarbon and oxygen will not be considered in depth. Interaction with anion vacancies on the titania surface is certainly involved, as it is in thermally induced oxidation reactions (*23*). The photoproduced holes and electrons react with surface oxygen (or hydroxyl) species, rather than with hydrocarbon, as shown by photoconductivity measurements (*10, 24*). As regards adsorption, however, the anion vacancy sites for oxygen and hydrocarbon adsorption may be identical. We shall as-

FIG. 2. The inverse rate of acetone formation from isobutane vs the inverse partial pressure of independent variable, for constant partial pressure of the second reactant. (a) Higher intensity case vs $(P_0)^{-1}$ (Fig. 7, Ref. *7*). (b) Higher intensity case vs $(P_0)^{-1/2}$ (Fig. 8, Ref. *7*). (c) Lower intensity case vs $(P_{O_2})^{-1}$. This figure contains all data in Fig. 4 of Ref. (*7*). The curves have been relabeled in the corrected order of oxygen partial pressure. P_0 = 7(○), 50(△), 250(x), and 310(◇) Torr.

sume such identity in the subsequent derivation; an analysis assuming separate adsorption sites will later be shown to be inconsistent with the data available.

The vacant site requirement for dehydration and the equality of steps 3a and 3b are characteristic of the reaction sequence we consider. Below we show that these kinetic features lead to rate expressions for both isobutane and 2-methyl-2-butyl-alcohol which agree with the published experimental data.

For the reactants in question, only one route to acetone exists, although oxygen insertion and alcohol dehydration do lead to other partial oxidation products. For isobutane, without indicating detailed mechanism(s),

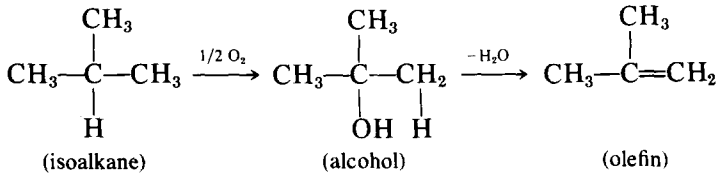

(9a)

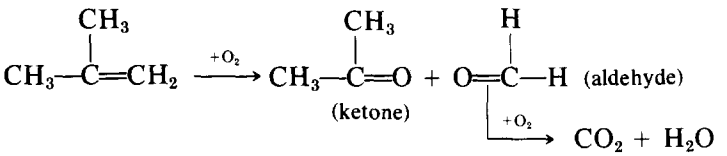

(9b)

For 2-methyl-2-butyl-alcohol,

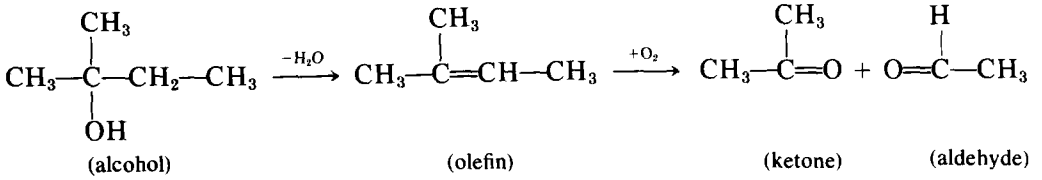

(10)

Assuming that dehydration is irreversible and rate determining, all subsequent steps are kinetically insignificant (*25*). At the conditions of these studies, acetone itself is not oxidized (*1, 8*). Therefore, the measured rate of acetone production is equal to the dehydration rate.

This rate is given by

$$r_{\text{acetone}} = r_{\text{dehydration}} = k_r \theta_{OH} \theta_v \qquad (11)$$

where θ_{OH} is the surface alcohol concentration and θ_v is the concentration of vacant sites. An explicit form of Eq. (11) may be derived for two cases, alcohol feed or alkane feed. In both cases, all sites are assumed to be indistinguishable.

Case I—Alcohol Feed

When alcohol is fed directly, the alcohol formation step is eliminated. Water was shown not to inhibit the reaction (*9*). Assuming both Langmuir adsorption of alcohol and oxygen and no product inhibition, the rate becomes

$$r_{\text{acetone}} = k_r \left[\frac{K_{OH}P_{OH}}{1 + K_{OH}P_{OH} + (K_O P_O)^N}\right] \left[\frac{1}{1 + K_{OH}P_{OH} + (K_O P_O)^N}\right]. \qquad (12)$$

The conversions for the alcohol oxidation range from ~3 to ~100%, requiring an integral analysis of the data. The low alcohol pressure points of Fig. 1b, at an oxygen

pressure of 608 Torr, represent essentially complete conversion, and consequently are useless for kinetic analysis. Only the data of Fig. 1a, for conversions of ~3 to ~79%, are suitable for an integral test of the model. As a result, the effect of oxygen pressure in Eq. (12) cannot be determined. As a first approximation, we assume the oxygen dependence to be weak, and neglect the term $(K_O P_O)^N$ with respect to unity in the denominator of Eq. (12). We return to this point later in the discussion. The rate expression becomes

$$r_{\text{acetone}} \cong \frac{k_r K_{OH} P_{OH}}{(1 + K_{OH} P_{OH})^2}. \quad (12a)$$

The change in number of moles due to reaction is neglected, since the highest conversions yield a volume change of only about 1% in this atmospheric reactor. The performance equation for a flow reactor, Eq. (13), may be integrated to yield Eq. (13a).

$$\frac{\text{catalyst mass}}{\text{volumetric flow rate}} = \frac{W}{v_0} = \left[\frac{-1}{RT}\right] \int_{P_{in}}^{P_{out}} \frac{dP_{OH}}{r_{\text{acetone}}} \quad (13)$$

$$\frac{k_r W}{v_0} = \frac{-1}{RT}\left\{\frac{1}{K_{OH}} \ln \frac{P_{out}}{P_{in}} + 2(P_{out} - P_{in}) + \frac{k_{OH}}{2}(P_{out}^2 - P_{in}^2)\right\}. \quad (13a)$$

The values of W and v_0 were reported as 0.008 g of TiO_2 and 40 ml/min, respectively. The outlet alcohol pressure is found by a mass balance on the reactants and products (see Table 1 reactions):

$$P_{OH}(\text{in}) - P_{OH}(\text{converted}) = P_{OH}(\text{out}) \quad (14a)$$

$$P_{OH}(\text{converted}) = P_{\text{acetone produced}} + P_{\text{butanone produced}}. \quad (14b)$$

From the inlet[1] and outlet pressures calculated in this manner, the constants of Eq. (13a) were evaluated by a nonlinear least-squares analysis. A trial and error solution of Eq. (13a) with those constants yielded calculated values of the outlet alcohol pressure. The average experimental ratio of acetone to butanone was used to convert the alcohol reacted to acetone produced,

$$P_{\text{acetone}} \cong (0.897)(P_{in} - P_{out}). \quad (15)$$

The outlet acetone pressure computed in this manner is compared to the experimental data of Fig. 1a in Fig. 3. The agreement is satisfactory: the curve calculated from this simple model retains the essential feature of the experimental data, i.e., the alcohol inhibition arising, according to our model, from inhibition of the dehydration step as the vacant site concentration is decreased.

The agreement of this model with experiment supports the hypothesis that two sites are needed for dehydration; we now extend the model to account for isobutane oxidation in Case II.

Case II—Alkane Feed

Formation of an alcohol from isobutane requires the early addition of a monotomic oxygen species. The alcohol coverage thus depends on two surface reactions in series: the formation and dehydration of alcohol. Again the assumption that all steps are fast compared to these two leads to a Langmuir adsorption term for the isobutane, and a pseudoequilibrium expression of similar form for the oxygen. Thus, assuming no product inhibition,

$$\theta_C = K_C P_C \cdot \theta_v \quad (16)$$

$$\theta_O = (K_O P_O)^N \cdot \theta_v \quad (17)$$

and

$$\theta_v = 1 - \theta_O - \theta_C - \theta_{OH}. \quad (18)$$

We emphasize that the oxygen coverage is not due to a simple chemisorption equilibrium, but represents a "pseudoequilibrium" which depends upon oxygen pres-

[1] Adjusting the inlet alcohol pressures from a room temperature (20°C) basis to a reaction temperature (95°C) basis assigns the conversion of the lowest inlet alcohol pressure to essentially 100%.

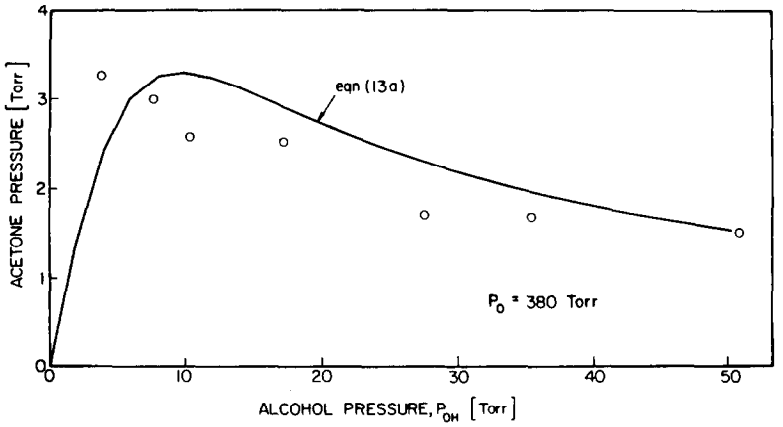

FIG. 3. Comparison of integral model calculation (Eq. 13a) and experiment for 2-methyl-2-butyl-alcohol oxidation (Case I). Solid lines are calculated with constants of Table 2.

sure, illumination intensity, quantum efficiency, and electron-hole recombination in the catalyst. The constant K_O should properly be considered as a "kinetic photoadsorption coefficient," to adapt Carberry's terminology (*26*) to photocatalytic reactions.

Following the alkane scheme in Table 1, a steady-state approximation on the alcohol coverage gives Eq. (19). (The back reaction rate constant, k_{-3}, is probably quite small since an alcohol may dehydrate or dehydrogenate but is not expected easily to deoxygenate.)

$$\frac{d\theta_{OH}}{dt} \cong 0 = k_3\theta_O\theta_C - (k_{-3} + k_4)\theta_{OH}\theta_v. \quad (19)$$

Here we again assume for simplicity that the predominant fate of the surface alcohol is dehydration, allowing neglect of the slower parallel path of desorption.

Solving Eqs. (16)–(19) simultaneously yields the surface coverages of interest:

$$\theta_{OH} = \left[\frac{k_3}{k_{-3} + k_4}\right] K_O{}^N K_C P_O{}^N P_C \cdot \theta_v \quad (20)$$

$$\theta_v = \frac{1}{1 + (K_O P_O)^N + K_C P_C + (k_3/(k_{-3} + k_4)) K_O{}^N K_C P_O{}^N P_C}. \quad (21)$$

Letting $\alpha \equiv k_3/(k_{-3} + k_4)$ and $\beta \equiv K_O{}^N K_C$, the rate of reaction becomes Eq. (22):

$$r_{acetone} = k_r\theta_{OH}\theta_v = \frac{k_r\alpha\beta P_O{}^N P_C}{(1 + (K_O P_O)^N + K_C P_C + \alpha\beta P_O{}^N P_C)^2}. \quad (22)$$

Inversion and rearrangement of Eq. (22) leads to expressions linear in P_C and $P_O{}^N$:

$$\left[\frac{P_O{}^N P_C}{r_{acetone}}\right]^{1/2} = I_c(P_O{}^N) + S_c(P_O{}^N)P_C \quad (23)$$

and

$$\left[\frac{P_O{}^N P_C}{r_{acetone}}\right]^{1/2} = I_{ON}(P_C) + S_{ON}(P_C)P_O{}^N. \quad (24)$$

The predicted dependence of these intercept (I) and slope (S) functions on reactant pressures is summarized in Table 3.

The isobutane conversions range from ~1 to ~8%, justifying a differential rate treatment of the data and neglect of the volume change due to reaction. Plots of

TABLE 2

Parameters for Eq. (12a) from Integral Analysis

$$r_{\text{acetone}} = \frac{k_r K_{OH} P_{OH}}{(1 + K_{OH} P_{OH})^2}$$

Conditions

Feed: 2-methyl-2-butyl-alcohol

T: 95°C

P_O: 308 Torr[a]

P_C: 0.76–51 Torr

Parameter values

k_r = 67.4 μmol/g · sec

K_{OH} = 0.133 Torr^{-1}

[a] 1 Torr = 1.33.3 N m^{-2}.

TABLE 3

Slope and Intercept Functions for the Rate Eqs. (23) and (24)

$$S_C = \frac{K_C}{(k_r\alpha\beta)^{1/2}} + \left(\frac{\alpha\beta}{k_r}\right)^{1/2} P_O^N$$

$$I_C = \frac{1}{(k_r\alpha\beta)^{1/2}} + \left(\frac{K_O^{2N}}{k_r\alpha\beta}\right)^{1/2} P_O^N \qquad \text{Eq. (23)}$$

$$S_{ON} = \left(\frac{K_O^{2N}}{k_r\alpha\beta}\right)^{1/2} + \left(\frac{\alpha\beta}{k_r}\right)^{1/2} P_C$$

$$I_{ON} = \left(\frac{1}{k_r\alpha\beta}\right)^{1/2} + \frac{K_C}{(k_r\alpha\beta)^{1/2}} P_C \qquad \text{Eq. (24)}$$

$$\alpha \equiv \frac{k_3}{k_{-3} + k_4} \qquad \beta \equiv K_O^N K_C$$

higher intensity isobutane oxidation data according to Eq. (24) are shown in Figs. 4a and b for $N = \frac{1}{2}$ and $N = 1$, respectively. As $N = \frac{1}{2}$ provides linear plots, only the case for dissociative oxygen adsorption will be considered further. The corre-

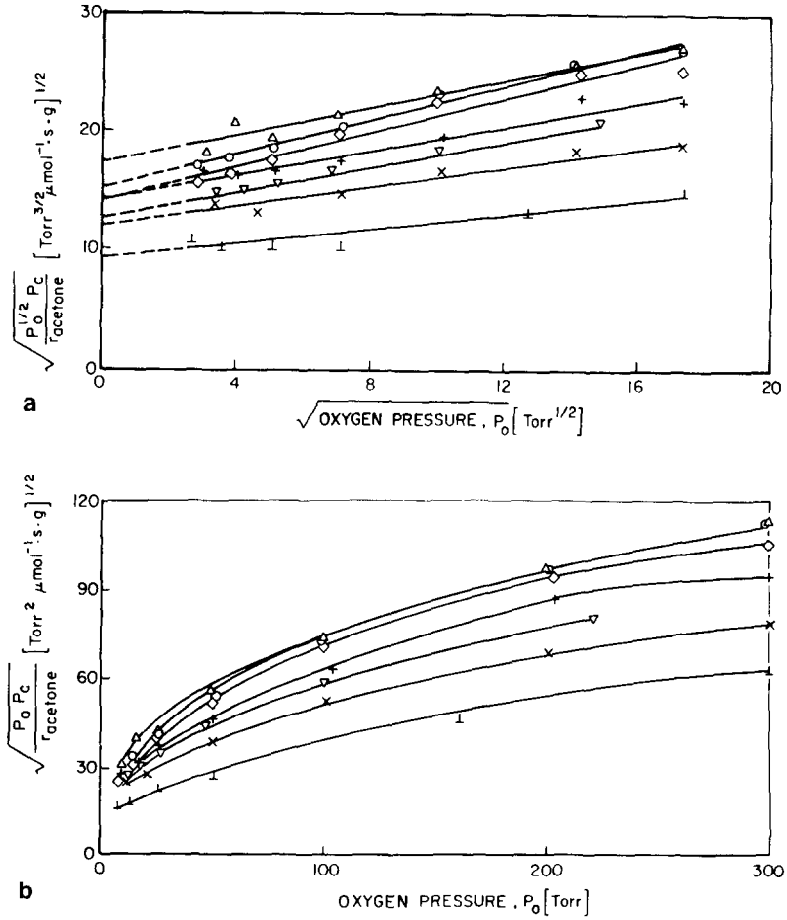

FIG. 4. Linearity test for isobutane oxidation with Eq. (24). Higher intensity. P_c = 7(⊥), 23(x), 36(▽), 60(+), 140(◇), 250(○), and 260(△) Torr. (a) $N = \frac{1}{2}$; (b) $N = 1$.

sponding plots of Eq. (23) at both higher and lower intensity are shown in Figs. 5a and b. Except for data below 40 Torr, the agreement is good.

The slopes (S_c) and intercepts (I_c) from a least-squares fit to the linear portions of Figs. 5a and b are plotted versus $(P_O)^{1/2}$ in Fig. 6. The corresponding values of $S_{O1/2}$ and $I_{O1/2}$ from Fig. 4a are plotted versus P_C in Fig. 7. Again the agreement with the linear behavior predicted by the model is satisfactory.

The constants of Eq. (22) were evaluated from the relationships in Table 3; their values appear in Table 4. The resulting Eq. (22) calculated with these constants is compared to the experimental data in Fig. 8. The agreement is satisfactory for the high intensity data, and less so for the data at a somewhat lower (unspecified) intensity.

Other simple models did not agree with the data. Assuming the sites in steps 3a and 3b to be distinguishable with separate site adsorption for oxygen and isobutane, yielded a rate expression which, in inverted form, had slope and intercept functions independent of the pressure of the second reactant, contrary to the data (*27*). Similarly, consideration of the alcohol formation step as the rate-determining process led to obviously incorrect predictions for either competitive or separate site adsorption.

The constants evaluated from our analysis are listed in Tables 2 and 4. Their relative values are informative. The 2-

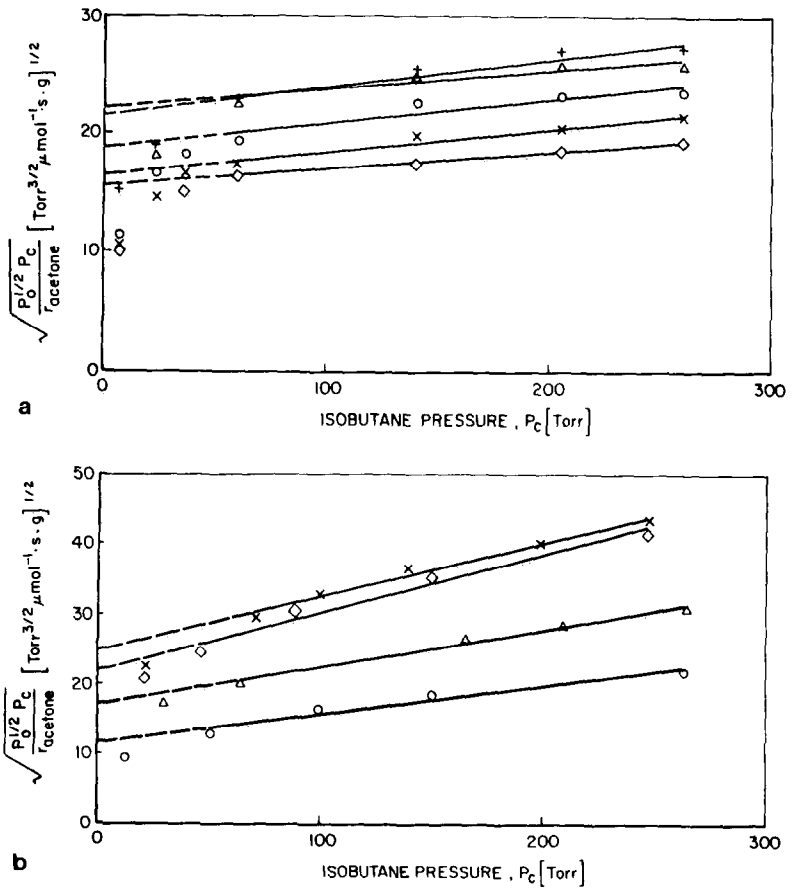

FIG. 5. Linearity test for isobutane oxidation model with Eq. (23). $N = \frac{1}{2}$. (a) Higher intensity—P_O = 26(◇), 50(x), 100(○), 201(△), 300(+) Torr; (b) Lower intensity—P_O = 7(○), 50(△), 260(x), 310(◇) Torr.

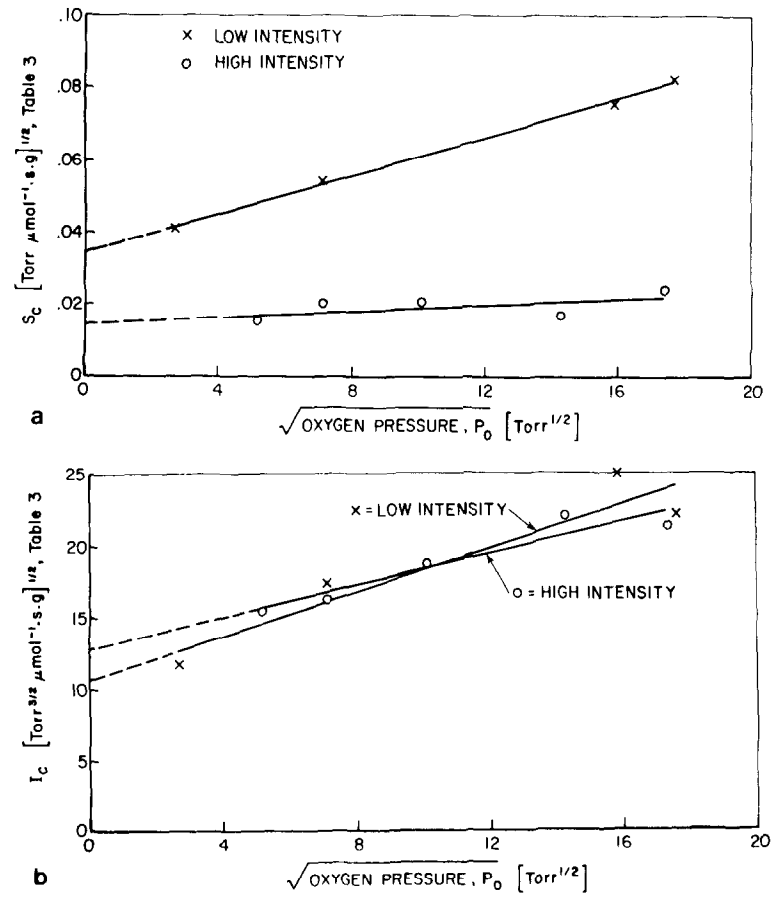

FIG. 6. Linearity test for slope and intercept functions from Eq. (23). Higher intensity (O). Lower intensity (x). (a) S_C vs $(P_O)^{1/2}$; (b) I_C vs $(P_O)^{1/2}$.

TABLE 4

Parameters for Eq. (22) from Differential Analysis[a]

$$r_{\text{acetone}} = \frac{k_r \cdot \alpha \cdot \beta P_O^{1/2} P_C}{[1 + (K_O P_O)^{1/2} + K_C P_C + \alpha\beta P_O^{1/2} P_C]^2}$$

Conditions: feed: isobutane illumination:	higher[b]	lower
T(°C):	30	30
P_O(Torr):	7–300	7–310
P_C(Torr):	7–260	7–300
Parameter values:		
k_r(μmol/g · sec):	172	34
K_O(Torr^{-1}):	1.9×10^{-3}	5.1×10^{-3}
K_C(Torr^{-1}):	1.15×10^{-3}	3.2×10^{-3}
α:	0.71	1.1
$\alpha\beta$(Torr$^{-3/2}$):	3.5×10^{-5}	2.6×10^{-4}

[a] $\alpha \equiv k_3/(k_{-3} + k_4)$, $\beta \equiv K_O^{1/2} K_C$.

[b] Parameter values determined from Eqs. (23) and (24), then averaged.

methyl-2-butyl-alcohol adsorption constant, K_{OH}, at 95°C is ≈100 times *larger* than K_C and K_O at 30°C. Thus $K_O P_O$ at 95°C is expected to be small, as we assumed in the Case I (alcohol oxidation) analysis. Similarly, K_{OH} for isobutyl-alcohol should be very large at 30°C, indicating that the presumed alcohol intermediate in Case II (isobutane oxidation) should be very strongly bound.

Inhibition by one alcohol at 95°C and lack thereof by the other at 30°C can be explained by calculating the coverages for typical experimental conditions. For alcohol oxidation, consider $P_{OH} = 10$ Torr, and for hydrocarbon oxidation, $P_O = P_C = 100$ Torr. At 95°C,

$$\theta_{OH} = \frac{K_{OH} P_{OH}}{1 + K_{OH} P_{OH}} \cong \frac{1.33}{2.33} \cong 0.57;$$

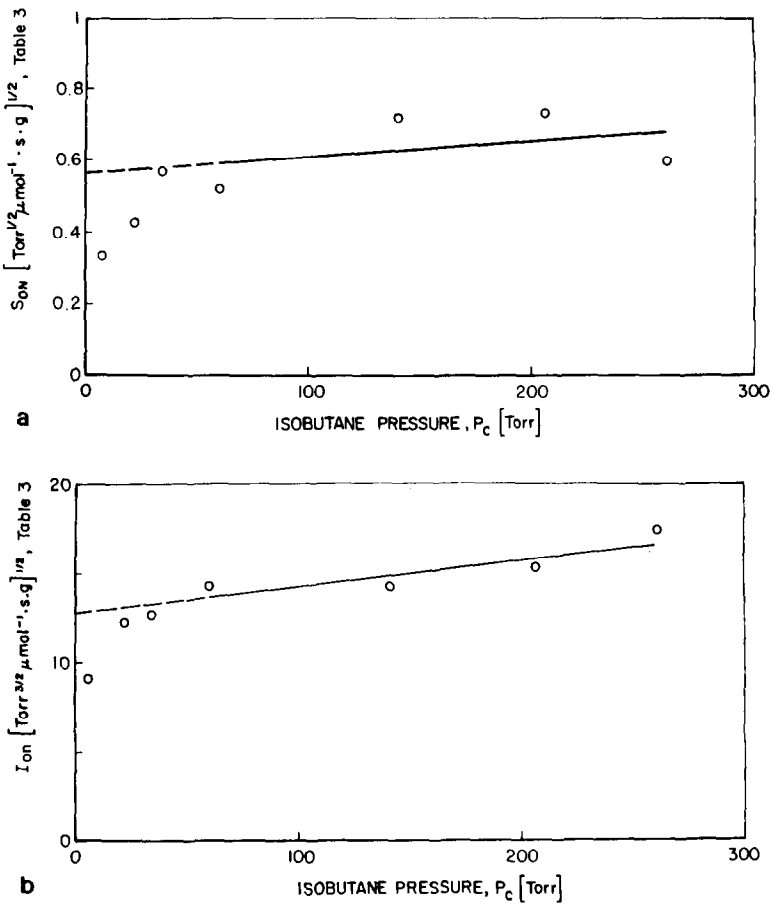

FIG. 7. Linearity test for slope and intercept functions from Eq. (24). Higher intensity, $N = \frac{1}{2}$. (a) S_{ON} vs P_C; (b) I_{ON} vs P_C.

at 30°C, from Eqs. (17), (18), (20), and (21),

$$\theta_O \approx 0.27,\ \theta_C \approx 0.07,$$
$$\theta_v \approx 0.63, \text{ and } \theta_{OH} \approx 0.02.$$

Inspection of Eq. (12a) shows that inhibition becomes apparent when $K_{OH}P_{OH} > 0.5$, i.e., when $\theta_{OH} > 0.5$.

For the isobutane oxidation, the strongly bound alcohol intermediate never accumulates to an inhibitory level. The values of α for the two isobutane experiments are near unity. If, as we earlier suggested, the value of k_{-3} is very small, then the forward rate constants for the two sequential bimolecular surface reactions, k_3 and k_4, are approximately equal. The alcohol coverage is maintained at a low level, $\theta_{OH} \approx 0.02$, since the rate of its formation from oxygen and isobutane is very close to the rate of its dehydration.

The rate constants, k_r, depend on intensity, as expected in light-consuming reactions. Although the present paper appears to improve the kinetic analysis of these photoassisted oxidations, it does not furnish new information about the light-induced step(s). Much research remains to be done before the dependence of the rate equation parameters on intensity, wavelength, and solid properties are determined experimentally in sufficient detail that theories for the connections between solid photoexcitation and surface catalysis can be seriously tested.

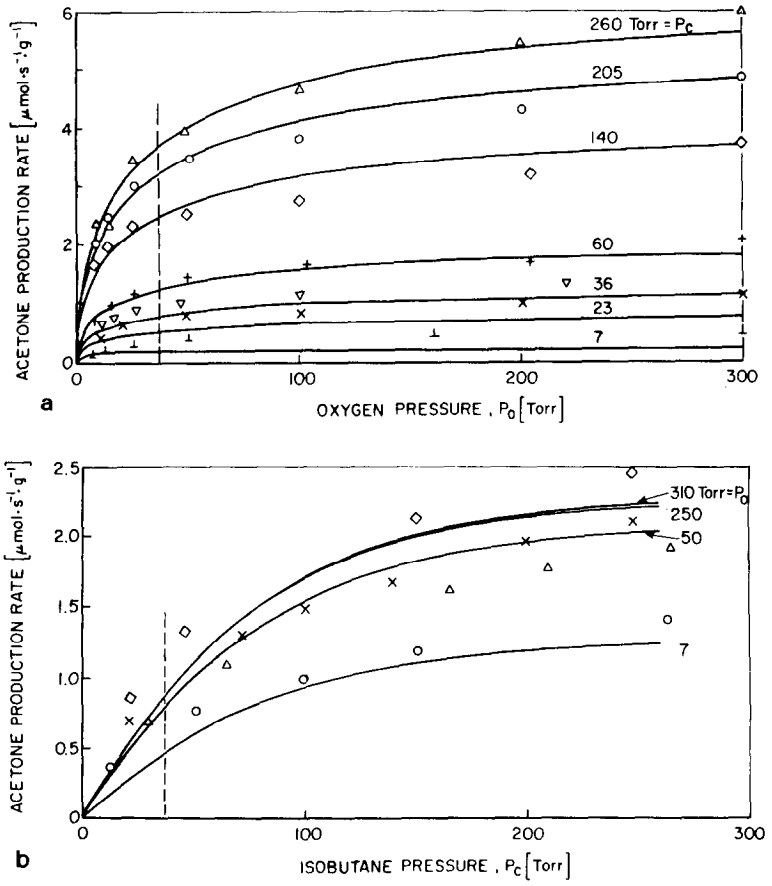

FIG. 8. Comparison of model calculations (Eq. 22) and experiment for isobutane oxidation (Case II). Solid lines are calculations with constants of Table 4. Data to the left of the vertical dashed lines were not included in evaluation of the constants. (a) Rate of acetone production vs P_O—higher intensity. (b) Rate of acetone production vs P_C—lower intensity.

CONCLUSION

Rate equations for the photoassisted catalytic oxidation of 2-methyl-2-butyl-alcohol and isobutane are proposed. For the alcohol oxidation, the kinetics can be described by assuming that the rate-determining step is the two-site dehydration of the alcohol. For the isobutane oxidation, two surface reactions in series are assumed to control the overall rate of acetone production. The first step involves formation of a surface alcohol intermediate from reaction of an adsorbed monatomic oxygen species and adsorbed alkane. The second step is assumed to be the two-site dehydration of adsorbed alcohol. The derivation presumes competition between the oxygen, hydrocarbon, and alcohol moieties for the vacant site required for dehydration.

The resultant expressions are consistent with reported dependencies of rate on pressures of all reactants (alcohol, alkane, and oxygen, as appropriate). The model equations are the first rate expressions developed for the photoassisted catalytic oxidation of hydrocarbons which account for intermediate formation. The oxygen dependency obtained herein supports the view that the oxygen participation is dissociative.

ACKNOWLEDGMENTS

LPC gratefully acknowledges her support by a Mo-

bil Incentive Fellowship, and useful discussions with J. C. Kantor, We are pleased to acknowledge support of the Engineering Foundation during portions of this study.

REFERENCES

1. Childs, L. P., and Ollis, D. F., *J. Catal.* **66**, 4891 (1980).
2. Formenti, M., Juillet, F., Meriaudeau, P., and Teichner, S. J., *Chem. Tech.* **1**, 680–686 (1971).
3. Gravelle, P., Juillet, F., Meriaudeau, P., and Teichner, S. J., *Disc. Faraday Soc.* **52**, 140–148 (1971).
4. Formenti, M., Juillet, F., Meriaudeau, P., and Teichner, S. J., *Bull. Soc. Chim. France* 69–76 (1972).
5. Djeghri, N., Formenti, M., Juillet, F., and Teichner, S. J., *Faraday Disc. Chem. Soc.* **58**, 185–193 (1974).
6. Juillet, F., LeComte, F., Mozzanega, H., Teichner, S. J., Thevenet, A., and Vergnon, P., *Faraday Symp. Chem. Soc.* **7**, 57–62 (1973).
7. Formenti, M., Juillet, F., and Teichner, S. J., *Bull. Soc. Chim. France* **7–8**, 1031–1036 (1976).
8. Formenti, M., Juillet, F., and Teichner, S. J., *Bull. Soc. Chim. France* **9–10**, 1315–1320 (1976).
9. Walker, A., Formenti, M., Meriaudeau, P., and Teichner, S. J., *J. Catal.* **50**, 237–243 (1977).
10. Hermann, J. M., Disdier, J., Mozzanega, M., and Pichat, P., 6th North American Meeting of the Catalysis Society, Chicago, March 1979; *J. Catal.* **60**, 369–377 (1979).
11. Bickley, R. I., and Stone, F. S., *J. Catal.* **31**, 389–397 (1973).
12. Bickley, R. I., Munuera, G., and Stone, F. S., *J. Catal.* **31**, 398–407 (1973).
13. Carrisoza, I., and Munuera, G., *J. Catal.* **49**, 174–188 (1977).
14. Carrisoza, I., and Munuera, G., *J. Catal.* **49**, 189–200 (1977).
15. Courbon, H., Formenti, M., and Pichat, P., *J. Phys. Chem.* **81**, 550–554 (1977).
16. Hinshelwood, C. N., "The Kinetics of Chemical Change," p. 208. Oxford University Press, Oxford, 1949.
17. Shelstad, K. A., Downie, J., and Graydon, W. A., *Canad. J. Chem. Eng.* **38**, 102–197 (1960).
18. Downie, J., Shelstad, K. A., and Graydon, W. A., *Canad. J. Chem. Eng.* **39**, 201–204 (1961).
19. Jaswal, I. S., Mann, R. F., Juusola, J. A., and Downie, J., *Canad. J. Chem. Eng.* **47**, 284–287 (1969).
20. Juusola, J. A., Mann, R. F., and Downie, J., *J. Catal.* **17**, 106–113 (1970).
21. Mars, P., and Van Kevelen, W., *Chem. Eng. Sci., Spec. Suppl.* **3**, 41–59 (1954).
22. Weisz, P. B., *J. Chem. Phys.* **21**, 1531–1538 (1953).
23. Gates, B. C., Katzer, J. R., and Schmit, G. C. A., "Chemistry of Catalytic Processes," pp. 337–349. McGraw-Hill, New York, 1979.
24. Herrmann, J. M., Disdier, J., and Pichat, P., "Proc. 7th Int. Vac. Congr. and 3rd Int. Conf. Solid Surfaces" (R. Dobrozemsky *et al.*, Eds.), Vol. II, p. 951. Vienna, 1977.
25. Boudart, M., *AIChE J.* **18**, 465–478 (1972).
26. Carberry, J. J., "Chemical and Catalytic Reaction Engineering," pp. 392–394. McGraw-Hill, New York, 1976.
27. A very recent paper (*10*) claimed that oxygen and isobutane do not competitively adsorb, based on some experiments in which these reactants were varied simultaneously. Since K_O and K_C in Table 4 are of the same order of magnitude, the experiments cited would provide a poor test for competition. The plots of inverse rate vs inverse pressure, to which we subjected the data of Ref. (*6*), provide a clear indication that a rate equation based on separate sites is inconsistent with the extensive rate data in Ref. (*6*).